



How JWST can measure first light, reionization and galaxy assembly

Rogier A. Windhorst^{a,*}, Seth H. Cohen^a, Rolf A. Jansen^a, Chris Conselice^b, Haojing Yan^b

^a Department of Physics and Astronomy, Arizona State University, Box 871504, Tempe, AZ 85287-1504, United States

^b California Institute of Technology, MS 100-22, Pasadena, CA 91125, United States

Available online 6 January 2006

Abstract

We summarize the design and performance of the James Webb Space Telescope that is to be launched to an L2 orbit in 2013, and how it is designed, in particular, to study the epochs of first light, reionization and galaxy assembly.

© 2005 Elsevier B.V. All rights reserved.

Keywords: James Webb Space Telescope; Population III stars; Reionization; Galaxy formation; Galaxy evolution

Contents

1. The James Webb Space Telescope and its instruments	113
2. Measuring first light, reionization and galaxy assembly	115
3. Conclusions and afterword	120
Acknowledgements	120
References	120

1. The James Webb Space Telescope and its instruments

The James Webb Space Telescope (JWST) is currently designed as a fully deployable 6.5 m segmented IR telescope, optimized for imaging and spectroscopy from 0.6 to 28 μm , to be launched by NASA in 2013 (Mather and Stockman, 2000) (<http://www.jwst.nasa.gov/>) and (<http://www.stsci.edu/jwst/>). After its launch – currently planned with an Ariane V – JWST will make a several month journey to the Earth–Sun Lagrange point L2. In route, JWST will be automatically deployed in phases, its instruments will be tested, and will be inserted into an L2 halo orbit. JWST has a nested array of sun-shields to keep its ambient temperature at $\lesssim 40$ K, allowing faint imaging (to $AB \lesssim 31.5$ mag or ≈ 1 nJy) and spectroscopy ($AB \lesssim$

29 mag) in the near- to mid-IR. From L2, JWST can cover the whole sky in segments that move along in RA with the Earth. It will have an observing efficiency $\gtrsim 70\%$, and send data back to Earth every day.

The Optical Telescope Element (OTE) of the 6.5-m JWST has 18 hexagonal mirror segments – each of 1.3 m diameter – and a total edge-to-edge diameter of 6.60 m. Its effective circular diameter is 5.85 m, and its effective collecting area is 25 m^2 . Instead of the original design of 36 smaller segments, the OTE design converged on 18 larger segments. This had both risk- and cost-benefits, was easier to construct, and provided better mid-spatial frequency OTE errors, resulting in better 1.0 μm performance. With only 18 mirror segments, one cannot cleanly descope the telescope aperture without doing major harm to its resulting PSF. Fig. 1(a) shows a simulation of the 6.5-m JWST PSF, and Fig. 1(b) shows a 20-h JWST simulation that reaches the HUDF depth. The JWST science requirements

* Corresponding author.

E-mail address: rogier.windhorst@asu.edu (R.A. Windhorst).

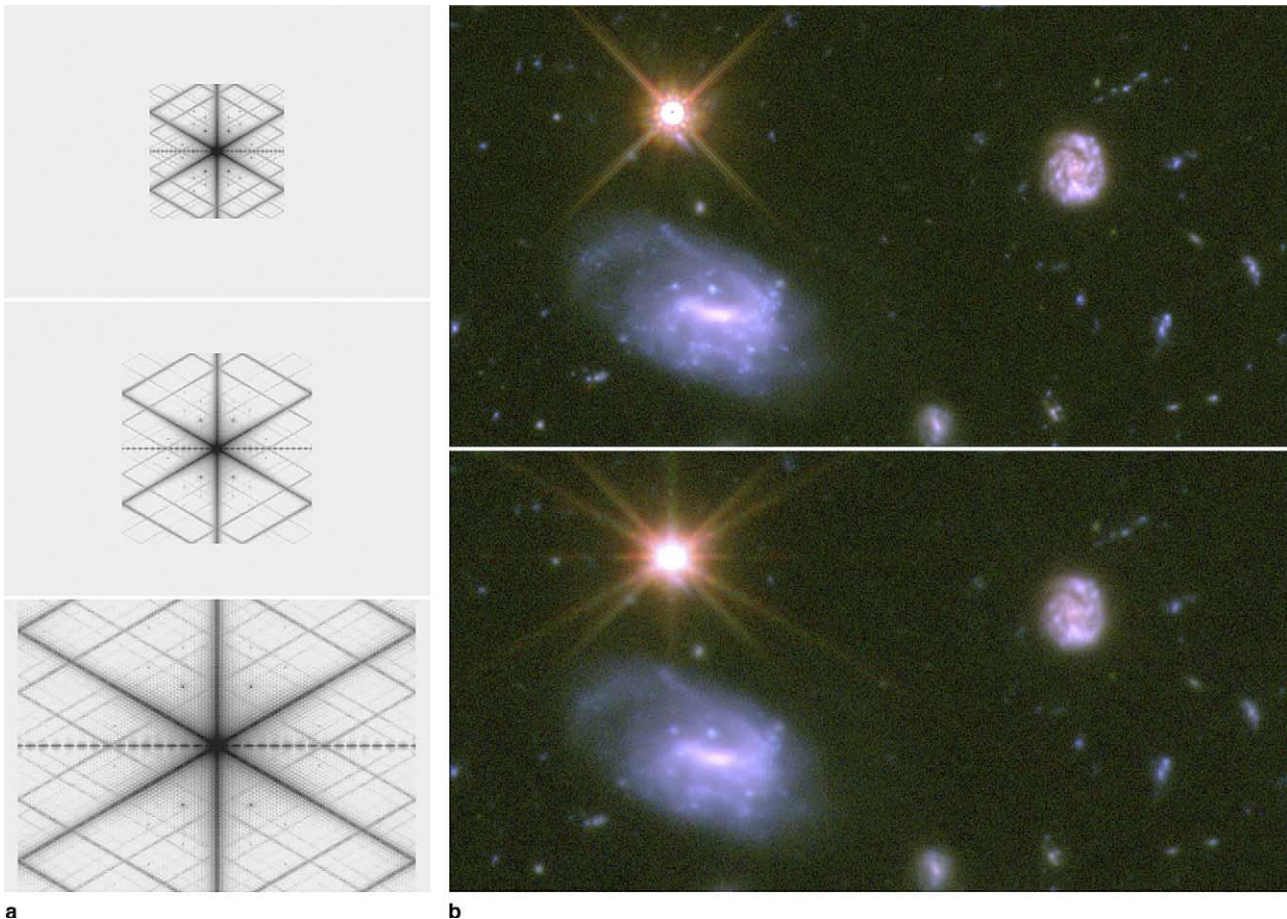


Fig. 1. (a) JWST PSF's at 0.7 μm (top), 1.0 μm (middle), and 2.0 μm (bottom), simulated by Ball Aerospace and GSFC for an OTE wave-front error WFE < 150 nm, corresponding to an encircled energy of EE = 74% inside a $r = 0.15''$ radius at 1.0 μm . (b) 240 h HST/ACS Vi'z' in the HUDF (top), and a JWST/NIRCam simulation at 0.7, 1.0, 2.0 μm , 20 h in total (bottom). The ACS PSF is ignored, resulting in two extra diffraction spikes for the bright star. The color image can be viewed at very high resolution from the PDF file on the website below. Even with a JWST PSF meeting current specs at 0.7 and 1.0 μm (74% EE inside $r = 0.15''$ at 1.0 μm), some loss in contrast is seen for faint "blue" objects. This is further quantified by Windhorst et al. (2003, 2005).

and its instruments are described by Gardner et al. (2004), Rieke et al. (2005), and on the websites listed in the references. In summary, JWST will have the following instruments:

- NIRCam:** The Near-Infrared Camera is made by an UofA + Lockheed + CSA consortium (<http://ircamera.as.arizona.edu/nircam/>). NIRCam will do imaging from 0.6 to 5.3 μm using a suite of broad-, medium-, and narrow-band filters. It uses two identical and independently operated imaging modules, with two wavelengths observable simultaneously via a dichroic that splits the beam around 2.35 μm . Each of these two channels has an independently operated 2.2' \times 4.6' field-of-view (FOV). Both channels are Nyquist-sampled: the short wavelength channel at 2.0 μm with 0.0317"/pixel, and the long wavelength at 4.0 μm with 0.0648"/pixel. NIRCam's ten 2k \times 2k HgCdTe arrays will be passively cooled. As shown below, a large FOV is essential to detect the expected first light objects.
- NIRSpec:** The Near-Infrared Spectrograph is made by an ESA + GSFC consortium (<http://www.stsci.edu/jwst/instruments/nirspec/>). NIRSpec will do spectroscopy with resolving powers of $R \sim 100$ in prism mode, of $R \sim 1000$ in multi-object mode using a micro-electro-mechanical array system (MEMS) of micro-shutters that can open slitlets on previously imaged known objects, and of $R \sim 3000$ using long-slit spectroscopy. All NIRSpec spectroscopic modes have a $\sim 3.4' \times 3.4'$ FOV. NIRSpec also has an IFU.
- MIRI:** The Mid-InfraRed Instrument is made by an UofA + JPL + ESA consortium (<http://ircamera.as.arizona.edu/MIRI/>). MIRI will do imaging and spectroscopy from 5 to 28 μm . It is passively cooled by a cryocooler instead of a cryostat, which would have only a 5-year lifetime. The NIRCam and MIRI sensitivity complement each other, straddling 5 μm in wavelength. To detect *and* confirm the first star-forming objects at redshifts $z \approx 15\text{--}20$ in $\gtrsim 10^5$ s (28 h) integration times, JWST needs both NIRCam at 0.6–5 μm and MIRI at 5–28 μm .

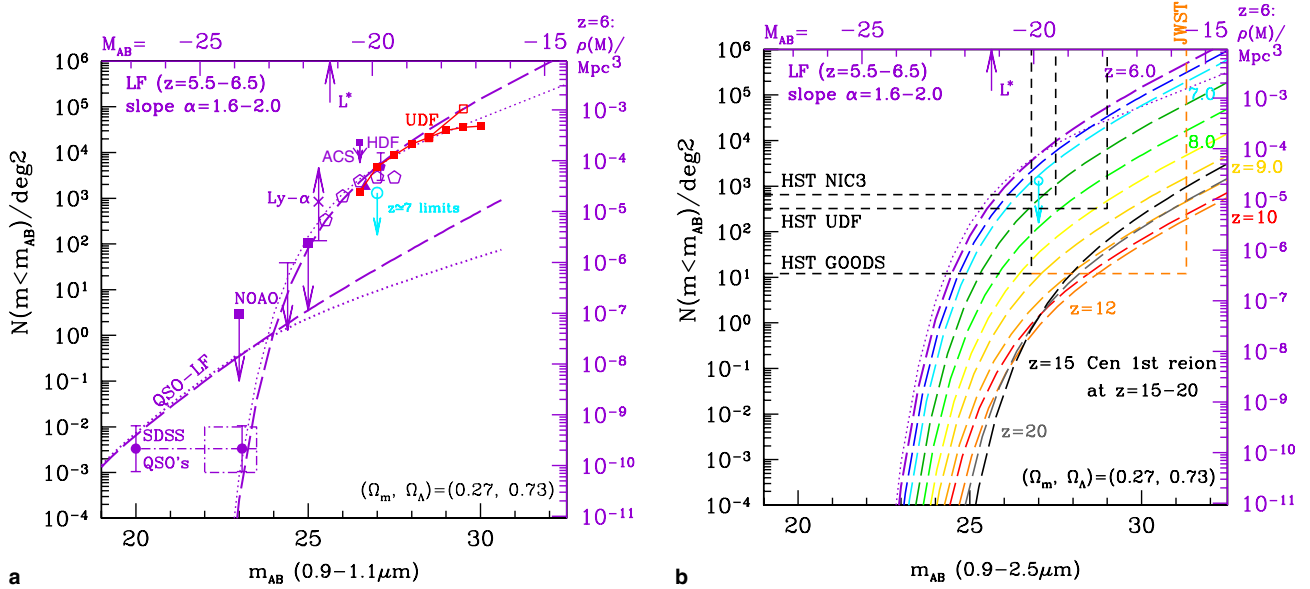


Fig. 2. (a) The HUDF suggested that the luminosity function (LF) of $z \approx 6$ objects may be very steep, with faint-end Schechter slope $|\alpha| \approx 1.8\text{--}1.9$ (Yan and Windhorst, 2004b). Dwarf galaxies and not quasars therefore likely completed the reionization epoch at $z \approx 6$ (Yan and Windhorst, 2004a). This is what JWST likely will observe in detail and to $AB = 31.5$ mag (1 nJy). (b) HST/ACS can detect objects at $z \lesssim 6.5$, but its discovery space $\mathcal{A} \cdot \Omega \cdot \Delta \log(\lambda)$ cannot trace the entire reionization epoch. NICMOS similarly is limited to $z \lesssim 8\text{--}10$. JWST can trace the entire reionization epoch from first light at $z \approx 20$ to the end of reionization at $z \approx 6$.

- **FGS:** The Fine Guidance Sensor is made by CSA and provides stable pointing at the milli-arcsecond level. It will have sufficient sensitivity and a large enough FOV to find guide stars with $\geq 95\%$ probability at any point in the sky. The FGS will have three simultaneously imaged fields of view of $3' \times 3'$, two of which feeds pure guider channels, while one feeds a guider channel plus a tunable-filter channel which will cover $1.7\text{--}4.7 \mu\text{m}$ at $R \sim 100$ resolution.

JWST has fully redundant imaging and spectroscopic modes. It will not be serviced at L2, and will undergo an extensive series of ground-testing and thermal vacuum testing in 2008–2009, after its main design and construction phase in 2004–2008. The main NASA contractor is Northrop Grumman Space Technology (“NGST”) in Redondo Beach (CA).

2. Measuring first light, reionization and galaxy assembly

- **First light:** The WMAP polarization results suggested that the universe was first reionized at redshifts as early as $z \approx 20$ (Spergel et al., 2003). This epoch of first light is thought to have started with Population III stars of $200\text{--}300 M_{\odot}$ at $z \approx 15\text{--}25$. These Pop III star clusters and their extremely luminous supernovae should be visible to JWST at $z \approx 15\text{--}25$. This epoch may have been followed by a delayed epoch of Pop II star-formation, since the Pop III supernovae may have sufficiently heated the IGM that it could not cool and form normal Pop II halo

stars until $z \approx 10$ (Cen, 2003). These halo Pop II stars may have formed in dwarf galaxies of mass $\approx 10^6\text{--}10^9 M_{\odot}$ with a gradual onset between $z \approx 10\text{--}6$. The reionization history may have been more complex and/or heterogeneous, with some Pop II stars forming in sites of sufficient density immediately following their Pop III predecessors. JWST is designed to detect the first super star-clusters and star-forming dwarf galaxies throughout the entire reionization epoch from $z \approx 20$ to $z \approx 6$, and measure their luminosity function (LF), as illustrated in Fig. 2(b), which is based on the double reionization model of Cen (2003). The surface densities at $z \approx 20$ were independently predicted by Stiavelli (2005, private communication), based on the models of Stiavelli et al. (2004). One must keep in mind that all these predictions are uncertain by at least 0.5 dex. Since in WMAP cosmology the amount of available volume per unit redshift decreases for $z \gtrsim 2$, the observed surface density of objects at $z \approx 10\text{--}20$ will be small, as shown in Fig. 2(b), depending somewhat on the exact hierarchical model predictions used. Hence, to observe the LF of first light star-clusters and subsequent dwarf-galaxy formation requires JWST to survey GOODS-sized areas to $AB = 31.5$ mag (≈ 1 nJy at $10\text{-}\sigma$), using seven filters for reliable photometric redshifts, since objects with $AB \gtrsim 29$ mag will be too faint for spectroscopy. With the 6.5-m JWST at its current specifications, such a survey requires 0.4 years of exposure time, i.e., even with the current 6.5 m JWST, this goes beyond an HST Treasury-sized program, and may require a dedicated multi-cycle community wide effort.

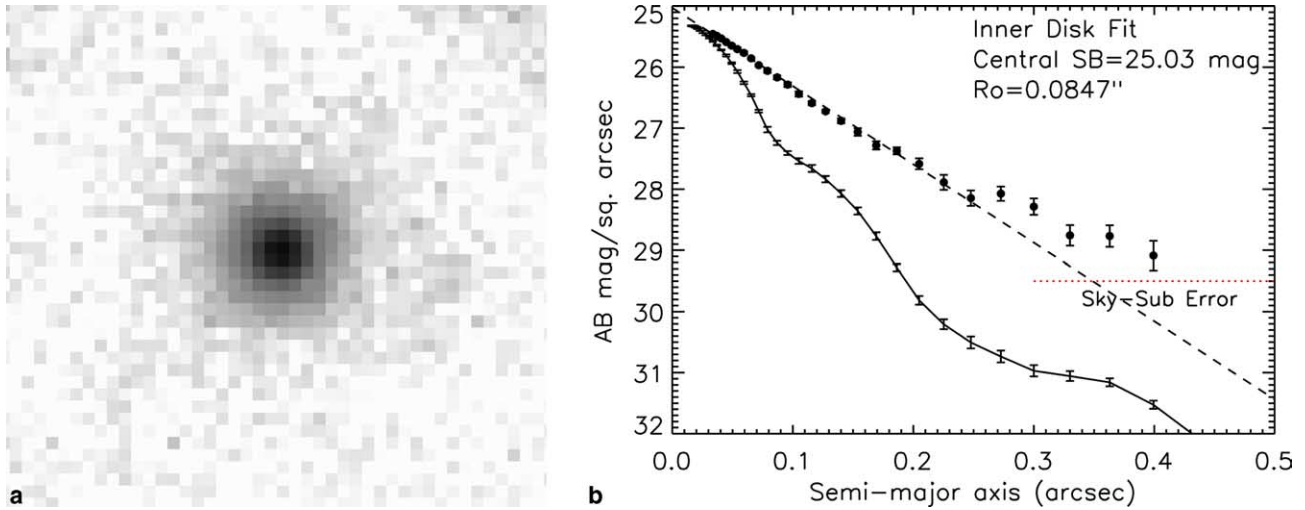


Fig. 3. (a) Sum of 49 compact isolated i-band dropouts in the HUDF (Yan and Windhorst, 2004b). This image is representative of a 5000-h HST z -band exposure – equivalent to a 330-h JWST $1\ \mu\text{m}$ exposure – of an average compact isolated $z \approx 6$ object. (b) The radial surface brightness (SB) profile of the image stack of (a). The physical radius where the profile starts to deviate from a pure exponential profile can be used as a dynamical clock (van Albada, 1982) to constrain their dynamical age, which is $\approx 100\text{--}200$ Myr at $z \approx 6$, i.e., similar to their SED age. HST cannot accurately measure individual objects at $z \approx 6$, but in long integrations JWST can measure the structure of the reionizing objects from $z \approx 20$ to $z \approx 6$.

- *Reionization:* The HUDF data suggested that the LF of $z \approx 6$ objects is potentially very steep (Bouwens et al., 2004; Yan and Windhorst, 2004b), with a faint-end Schechter slope $|\alpha| \approx 1.8\text{--}1.9$ after correcting for incompleteness of the ACS i-band dropout samples (Fig. 2(a)). Deep HST/ACS grism spectra confirmed 85–93% of the HUDF i-band dropouts to $\text{AB} = 27$ mag to be at $z \approx 6$ (Malhotra et al., 2005). The steep faint-end slope of the $z \approx 6$ LF implies that dwarf galaxies may have collectively provided enough UV-photons to complete reionization at $z \approx 6$ (Yan and Windhorst, 2004a). This assumes that the Lyman continuum escape fraction at $z \approx 6$ is as large as observed in Lyman Break Galaxies at $z \approx 3$, which is reasonable – although not proven – given the expected low dust content in dwarf galaxies at $z \approx 6$. Hence, dwarf galaxies, and not quasars, likely completed the reionization epoch at $z \approx 6$. The Pop II stars in dwarf galaxies cannot have started shining *per se* much before $z \approx 7\text{--}8$, or no neutral H-I would be seen in the foreground of $z \gtrsim 6$ quasars (Fan et al., 2003), and so dwarf galaxies may have ramped up their formation fairly quickly from $z \approx 10$ to $z \approx 6$. A first glimpse of this may already be visible in the NIC3 surveys of the HUDF, which suggests a significantly lower surface density of $z \gtrsim 7$ candidates compared to $z \approx 6$ objects (Bouwens et al., 2004b; Yan and Windhorst, 2004b light blue upper limit in Fig. 2(a) and (b)), although the $\gtrsim 600$ HST orbits spent on the HUDF only resulted in a few $z \gtrsim 7$ candidates at best.

HST/ACS can detect objects at $z \lesssim 6.5$, but its discovery space $A \cdot \Omega \cdot \Delta \log(\lambda)$ cannot trace the entire reionization epoch. HST/NICMOS similarly is limited to $z \lesssim 8\text{--}10$ and has very limited statistics. HST/WFC3 –

if it gets launched – will be able to explore the same redshift space, but with a wider FOV than NICMOS/NIC3. Fig. 2 shows that with proper survey strategy (area and depth), JWST can trace the entire reionization epoch from first light at $z \approx 20$ to the end of the reionization epoch at $z \approx 6$. Hence, JWST can trace the entire reionization epoch, by detecting the first star-forming objects, and measure their LF and its evolution. For this to be successful in realistic or conservative model scenarios, JWST needs to have the quoted sensitivity/aperture (“ A ”; to reach $\text{AB} \gtrsim 31$ mag), field-of-view ($\text{FOV} = \Omega$; to cover GOODS-sized areas), and wavelength range ($0.7\text{--}28\ \mu\text{m}$; to cover SED’s from the Lyman to Balmer breaks at $z \gtrsim 6\text{--}20$), as summarized in Fig. 2(b).

Fig. 3(a) shows the sum of 49 compact isolated i-band dropouts in the HUDF (Yan and Windhorst, 2004b), which is a stack of about half the $z \approx 6$ objects that have no obvious interactions or neighbors. These objects all have similar fluxes and half-light radii (r_e), so this image represents a 5000-h HST/ACS z -band exposure on an “average compact isolated $z \approx 6$ object”, which is equivalent to a ~ 330 -h JWST $1\ \mu\text{m}$ exposure on *one* such object. Fig. 3(b) shows that the radial SB-profile of this stacked image deviates from a pure exponential profile for $r \gtrsim 0.25''$, at SB-levels that are well above those corresponding to the $3\text{-}\sigma$ limits due to PSF and sky-subtraction errors. In hierarchical models, this physical scale-length is a direct dynamical clock (e.g., van Albada, 1982), constraining the dynamical age of these compact isolated i-band $z \approx 6$ dropouts to $\approx 100\text{--}200$ Myr, i.e., similar to their stellar population age.

This then suggests that the bulk of their stars observed at $z \approx 6$ may have started forming around $z_{\text{form}} \approx 7.0 \pm 0.5$. In the light of WMAP results, this is

consistent with the double reionization model of Cen (2003), where the first reionization by Pop III stars at $z \approx 10$ –20 is followed by a delayed onset of Pop II star-formation in dwarf galaxies at $z \lesssim 10$. HST cannot accurately measure individual light-profiles at $z \approx 6$, but in long integrations JWST can measure the growth of objects from the onset of reionization at $z \approx 20$ to its end at $z \approx 6$.

- *Galaxy assembly*: One of the remarkable discoveries of HST was how numerous and small faint galaxies are (Abraham et al., 1996; Driver et al., 1995; Glazebrook et al., 1995; Pascarella et al., 1996). They are likely the building blocks of the giant galaxies seen today. Galaxies with types on the present-day Hubble sequence formed over a wide range of cosmic time, but with a notable phase transition around $z \approx 1$: (1) Subgalactic units rapidly merge from $z \approx 7$ to $z \approx 1$ to grow bigger units; (2) Merger products start to settle as galaxies with giant bulges or large disks around $z \approx 1$. These evolved mostly passively since then (as tempered by the cosmological constant, see e.g., Cohen et al., 2003), resulting in the giant galaxies that we see today. JWST can measure how galaxies of all types formed over a wide range of cosmic time, by accurately measuring their distribu-

tion over rest-frame type and structure as a function of redshift or cosmic epoch (see Figs. 4 and 5).

Fig. 4 illustrates how Fourier Decomposition of nearby galaxies seen with HST in the rest-frame UV can be used to quantitatively measure bars, rings, spiral arms, and other structural features (e.g., Odewahn et al., 2002). Fourier Decomposition is remarkably good in distinguishing and quantifying bars and (1-armed, 2-armed) spiral structure. Observing distant galaxies in deep JWST NIRC*am* images will in a similar fashion directly trace the evolution of bars, rings, spiral arms, and other structural features in these objects, which will be anchored in the rest-frame UV images of the same structures seen in nearby galaxies (Windhorst et al., 2002). This will allow JWST to measure the detailed history of galaxy assembly in the epoch $z \approx 1$ –3, when most of today’s giant galaxies were made.

The uncertain rest-frame UV-morphology of galaxies is dominated by young and hot stars, with often copious amounts of dust superimposed. This will complicate the study of NIRC*am* images of very high redshift galaxies, but the longer wavelengths from MIRI will help constrain the effects from dust. With good images, a quantitative analysis of the restframe-wavelength dependent

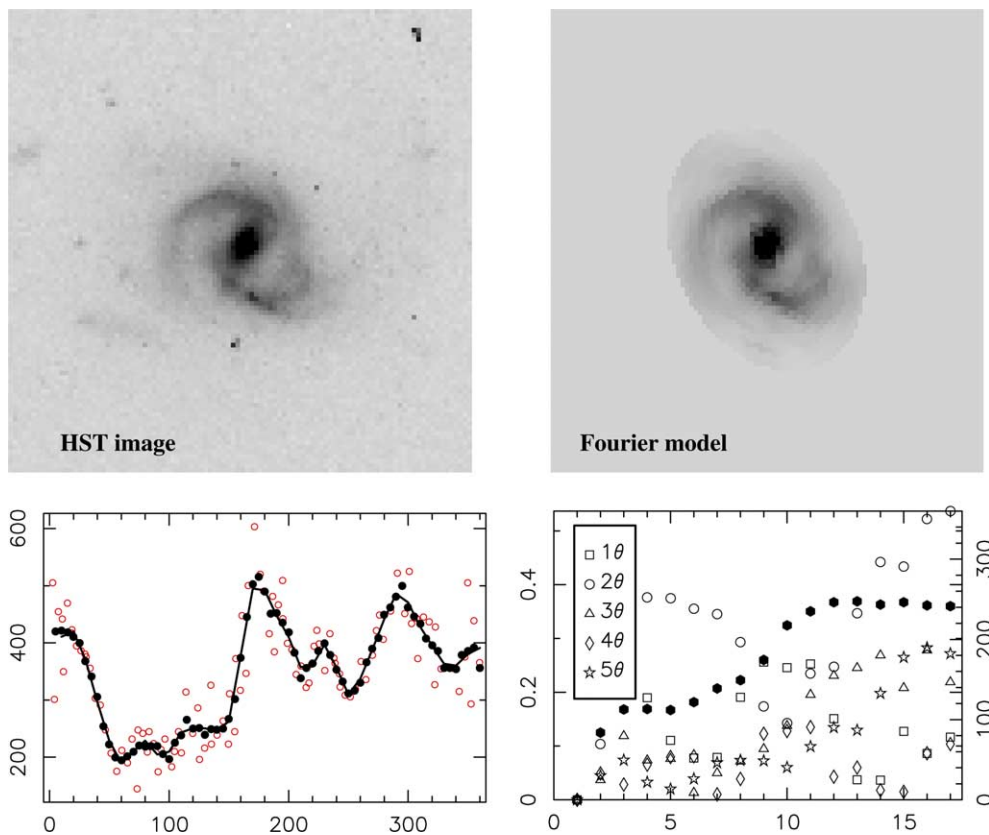


Fig. 4. Fourier decomposition (FD) is a robust way to measure galaxy structure and morphology in a quantitative way (c.f., Odewahn et al., 2002). FD decomposes a real image (top left) into Fourier series in successive concentric annuli (bottom left), resulting in an accurate decomposition (top right) that turns $\sim 100^2$ pixels (top left) into less than a 100 numbers (bottom right). The even Fourier components indicate symmetric galaxy parts (arms, rings), while the odd Fourier components indicate asymmetric parts (bars, etc.). Its large wavelength range allows JWST to measure the evolution of each physical feature directly.

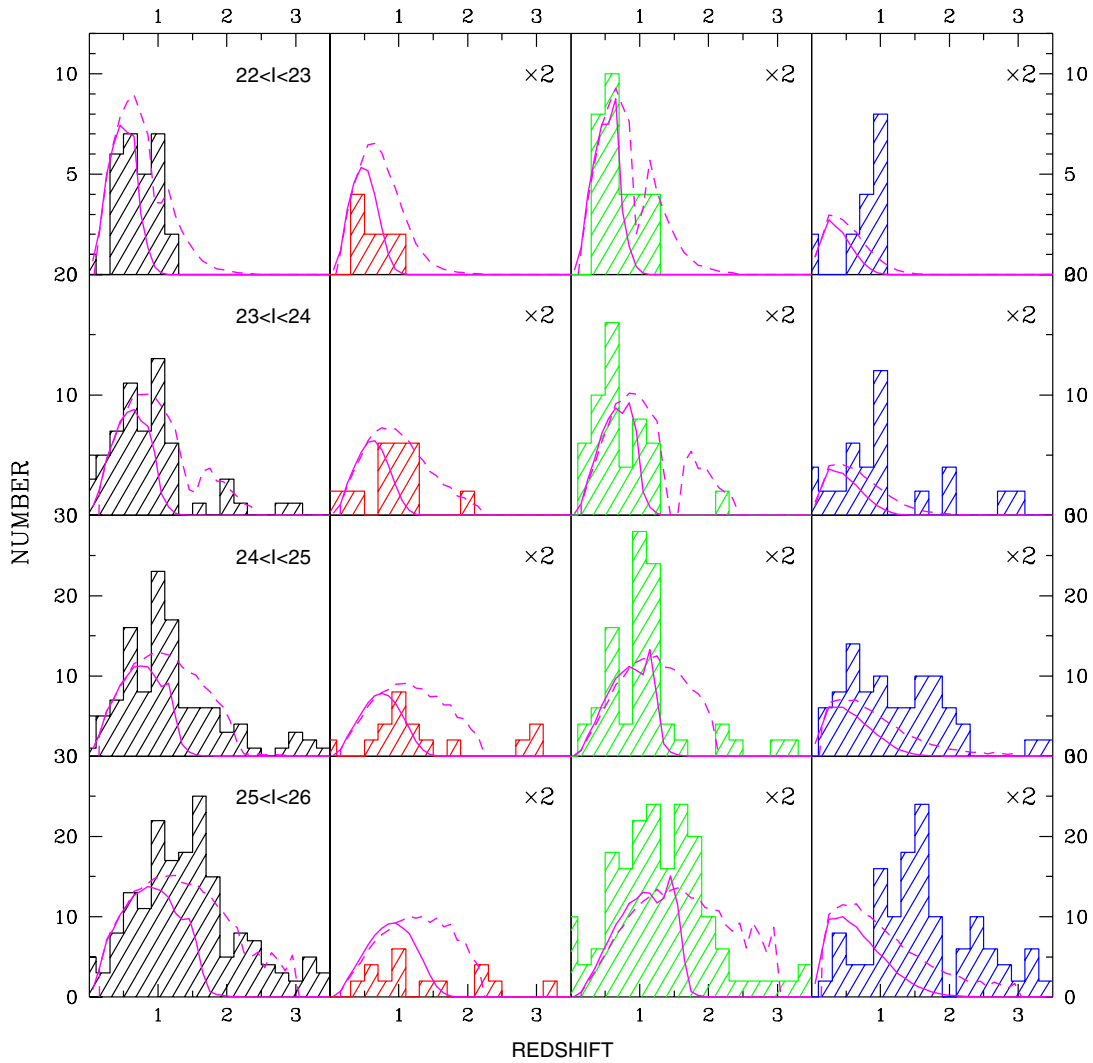


Fig. 5. JWST can measure how galaxies of all Hubble types formed over a wide range of cosmic time, by measuring their redshift distribution as a function of rest-frame type (e.g., Driver et al., 1995). These are shown here for all objects (black histograms in left column), early types (E/S0; red histograms), mid-type spirals (Sa–Sc; green histograms), and late-types (Scd–Im/Pec; blue histograms). JWST “types” will not only include galaxy morphology or Hubble class – which is poorly determined at $z \geq 1$ – but also physical structures, such as disks, spiral arms, bars, asymmetry, clumpiness, etc., as determined by Fourier decomposition (Fig. 4). (For interpretation of the references to colour in this figure legend, the reader is referred to the web version of this article.)

morphology and structure can be then made (e.g., Odewahn et al., 2002). JWST can measure how galaxies of all Hubble types formed over a wide range of cosmic time, by measuring their redshift distribution as a function of rest-frame type (Driver et al., 1995; Fig. 5). For this to work, the galaxy structure must be well imaged for large samples from deep, uniform and high quality multi-wavelength images, which JWST can do through dedicated surveys.

Spatially resolved NIRSpec and MIRI integral-field spectra of distant galaxies – when compared to the quantitative structure from NIRCам Fourier Decompositions – will allow to directly trace the physical causes of locally enhanced star-formation: infall, bulk velocities in excess of regular rotation, etc., and so map galaxy assembly in detail. For the sake of space, the detailed spatially resolved spectroscopic studies of

distant galaxies possible with JWST NIRSpec and MIRI are not reviewed here, but readers are referred to, e.g., Lilly et al. (1998) and Abraham et al. (1999) as to how such studies have been done in the past, and to the websites in the References as to how JWST will address the mass assembly of galaxies in this manner more quantitatively, and at much higher redshifts.

Fig. 6 shows how – with proper restframe-UV templates and training – JWST can quantitatively measure the evolution of galaxy morphology and structure over a wide range of cosmic time. These JWST simulations show that: (1) Most grand design disks become invisible due to SB-dimming at very high redshifts ($z \approx 15$ – 20), but they likely formed at $z \approx 1$ – 2 anyway; (2) High-SB structures in star-forming objects and mergers/train-wrecks are visible to $z \approx 10$ – 15 ; (3)

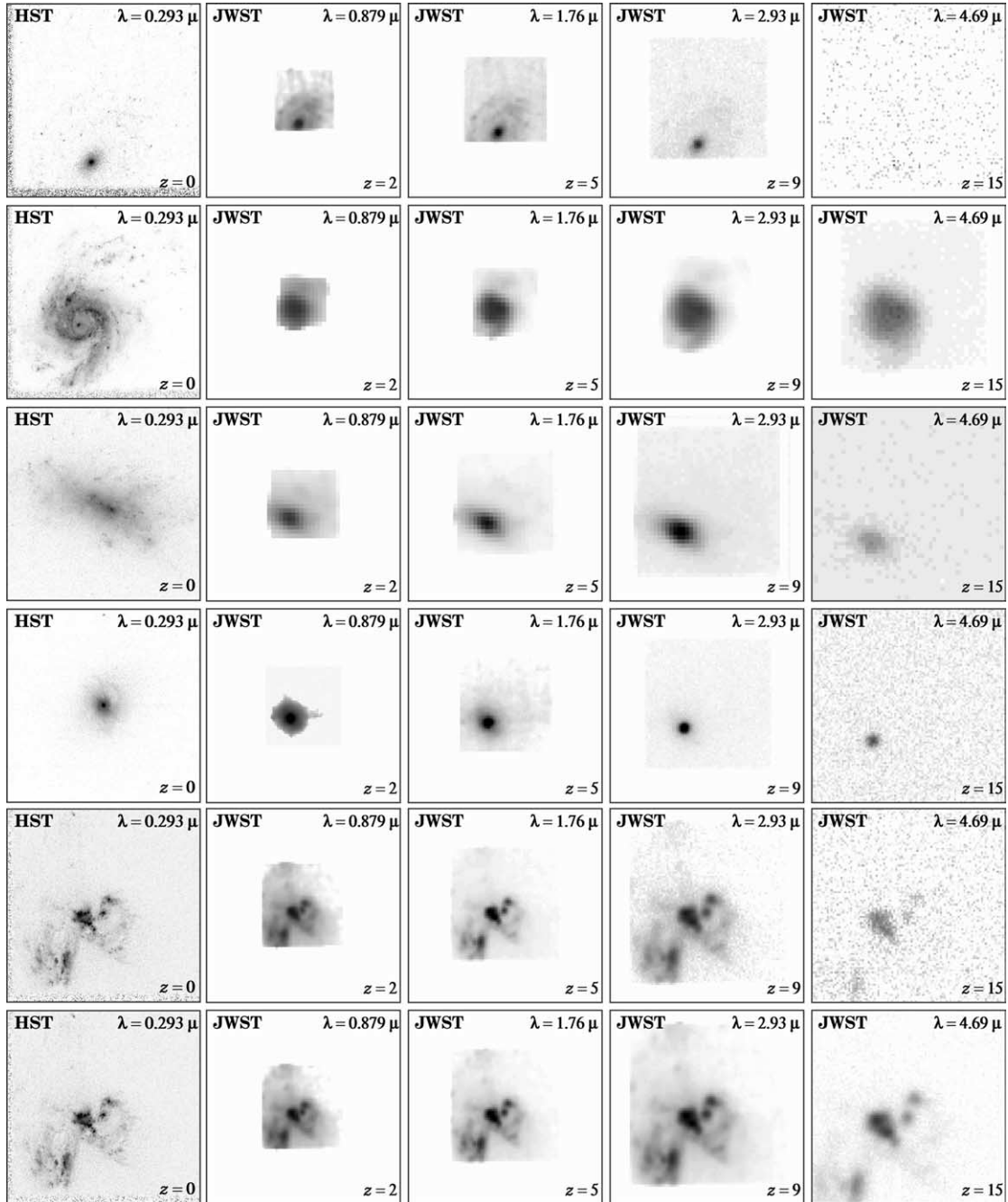


Fig. 6. Rows 1–5 show 1-h JWST NIRCcam simulations of nearby galaxies observed with HST/WFPC2 in the mid-UV (Windhorst et al., 2002). Row 6 is a 100-h simulation of JWST fully built to its specifications. The HST images (left column) are $37''$ or $75''$ across, and the JWST images $0.7''$ – $3.0''$. The rows show that: (Row 1) Most disks will SB-dim away at high z (but most disks formed at $z \approx 1$ – 2 anyway); (Rows 2–3 and 5–6) High SB structures in star-forming objects and mergers/train-wrecks are visible to very high z ; (Row 4) Point sources (weak AGN) are visible to very high z . The two high-SB clumps in the upper right of the merger in Rows 5–6 have $\sim 10^8$ – $10^9 M_{\odot}$ in stars, and are more representative of the objects that JWST can detect at $z \gtrsim 10$. Deep JWST surveys can quantitatively measure the evolution of galaxy structure and morphology over the entire epoch of galaxy assembly.

Point sources (e.g., Pop III star clusters and weak AGN) are visible to $z \approx 15$ – 20 . With proper rest-frame-UV training, deep JWST surveys can thus quantitatively measure the evolution of galaxy structure and morphology over the entire epoch of galaxy assembly (i.e., from $z \approx 15$ to $z \approx 1$).

These simulations do not imply that observing star-forming objects at $z \gtrsim 10$ with JWST will be easy.

On the contrary, since galaxies formed through hierarchical merging, many objects at $z \approx 10$ – 15 will be 10^1 – $10^4 \times$ less luminous than the actively star-forming objects seen with HST nearby, hence require pushing JWST to its very limits. Beyond $z \gtrsim 10$ – 12 , the cosmological SB-dimming will also render most of the lower-SB flux in objects invisible, except in the longest JWST integrations, as shown in row 6 of Fig. 6.

3. Conclusions and afterword

In summary, to have a decent chance of measuring the LF of the first star-forming objects at $z \approx 10\text{--}20$ will require very long integrations to $AB = 31.5$ mag over a GOODS-sized field with the 6.5-m JWST (Fig. 2(b)). It is therefore important in the current definition and re-planning of JWST, to keep its primary goals of detecting first light in mind.

It is in this context prudent to briefly reflect on the history of JWST. Shortly after the first stunning refurbished HST results appeared in 1994, AURA prompted the community to outline what the future of space imaging should look like. This resulted in the “HST and Beyond” study (Dressler et al., 1996) supported by NASA. This committee recommended a large (4 m) Infrared-Optimized Space Telescope, then referred to as the Next Generation Space Telescope (NGST). The NASA Administrator Dan Goldin subsequently told the community to think big, and consider a 6–8-m deployable NGST. In the mid-late 1990s, the earlier Adhoc and Interim NGST Science Working Groups then outlined an initial science program and requirements for the 8-m NGST (Stockman et al., 1997). Meanwhile, theory had sufficiently progressed to argue that the epoch of first light may have occurred at very high redshifts, and part of the science case in the NGST Design Reference Mission was developed to reflect this. The 8-m NGST concept was endorsed with top priority by the Decadal National Academy of Sciences survey (McKee and Taylor, 2001).

In 2002, TRW (now Northrup-Grumman Systems or NGS) had the winning proposal with a 7.0-m NGST, which was awarded the NASA contract. Then realism set in, and in late 2002, NASA and the Flight Science Working Group (SWG) worked together to define the currently designed 6.5-m telescope, named the James Webb Space Telescope in 2002. In early 2003, the WMAP polarization results suggested that first light may have occurred through Pop III stars as early as $z \approx 20$. While the error bars on this result still have to come down and its redshift range refined (Wright et al., 2005), the Fe-lines seen in $z \approx 6$ quasars by Freudling et al. (2003) also suggested a very early epoch of star-formation and supernovae. In the last few years, the *Spitzer Space Telescope* (2004) has shown us beautiful results underscoring the critical role of dust in galaxies and optically hidden star-formation at high redshifts, as shown in the special 2004 ApJ Suppl. Spitzer issue (e.g., Werner et al., 2004).

In conclusion, if the JWST is to remain NASA’s first light machine, it needs to have a 6.5-m class aperture and its near-IR to mid-IR capabilities to assure proper measurement of the expected first light objects. In a sense, JWST needs to combine the best of HST and Spitzer and fold this into a mission that can successfully open the next major frontier in astronomy.

Acknowledgements

The HST work was supported by Grants GO-8645.* and GO-9780.* from STScI, which is operated by AURA

for NASA under contract NAS 5-26555. The JWST work was supported from NASA JWST Grant NAG 5-12460. RAW thanks the other members of the JWST Flight Science Working Group, the JWST Instrument Teams, and the JWST hardware teams for their continuous dedicated work on the JWST project. A PDF file of the review presented at the conference is available at: www.physics.uci.edu/Cosmology/#schedule. This paper and other JWST studies are also available as PDF files at: www.asu.edu/clas/hst/www/jwst/.

References

- Abraham, R.G. et al., 1996. MNRAS 279, L47.
 Abraham, R.G. et al., 1999. MNRAS 303, 641.
 Bouwens, R.J. et al., 2004a. ApJL 606, L25.
 Bouwens, R.J. et al., 2004b. ApJL 616, L79.
 Cen, R., 2003. ApJ 591, 12.
 Cohen, S.H. et al., 2003. AJ 125, 1762 astro-ph/0301187.
 Dressler, A. et al., 1996. Report to NASA from the “HST and Beyond” Committee. AURA, Washington, DC.
 Driver, S.P. et al., 1995. ApJ 449, L23.
 Fan, X. et al., 2003. AJ, 125.
 Freudling, W., Corbin, M.R., Korista, K.T., 2003. ApJL 587, L67.
 Gardner, J., Mather, J., Clampin, M., Greenhouse, M., Hammel, H., Hutchings, J., Jakobsen, P., Lilly, S., Lunine, J., McCaughrean, M., Mountain, M., Rieke, G., Rieke, M., Smith, E., Stiavelli, M., Stockman, H., Windhorst, R., Wright, G., 2004. JWST Flight Science Working Group, Proc. SPIE 5487, 564.
 Glazebrook, K. et al., 1995. MNRAS 275, L19.
<http://ircamera.as.arizona.edu/nircam/>.
<http://ircamera.as.arizona.edu/MIRI/>.
<http://www.jwst.nasa.gov/>.
 Lilly, S.J. et al., 1998. ApJL 500, L75.
 Malhotra, S. et al., 2005. ApJ 626, 666.
 Mather, J., Stockman, H., 2000. In: Breckinridge, J.B., Jakobsen, P. (Eds.), UV, Optical, and IR Space Telescopes and Instruments, SPIE, 4013, 2. Springer, Berlin.
 McKee, C.F., Taylor, J.H., 2001. Astronomy and Astrophysics in the New Millennium. National Academy Press, Washington.
 Odewahn, S.C. et al., 2002. ApJ 568, 539.
 Pascarelle, S.M. et al., 1996. Nature 383, 45.
 Rieke, M.J. et al., 2005. In: Cooray, A., Barton, E., (Eds.), Proceedings of the UC Irvine Workshop on First Light and Reionization: Theoretical Study and Experimental Detection of the First Luminous Sources, New Astron. Rev. (this volume).
 Spergel, D.N. et al., 2003. ApJS 148, 175.
 Spitzer Space Telescope, First Observations, 2004. ApJS 154, 1–472.
<http://www.stsci.edu/jwst/>.
<http://www.stsci.edu/jwst/instruments/nirspec/>.
 Stiavelli, M., Fall, S.M., Panagia, N., 2004. ApJL 610, L1.
 Stockman, H.S. et al., 1997. The Next Generation Space Telescope, Visiting a Time when Galaxies were Young. AURA, Washington, DC.
 van Albada, T.S., 1982. MNRAS 201, 939.
 Werner, M.W. et al., 2004. ApJS 154, 1.
 Windhorst, R.A. et al., 2002. ApJS 143, 113.
 Windhorst, R.A. et al., 2003, 2005. www.asu.edu/clas/hst/www/jwst/.
 Wright, N., et al., 2005. In: Cooray, A., Barton, E., (Eds.), Proceedings of the UC Irvine Workshop on First Light and Reionization: Theoretical Study and Experimental Detection of the First Luminous Sources, New Astron. Rev. (this volume).
 Yan, H., Windhorst, R., 2004a. ApJL 600, L01.
 Yan, H., Windhorst, R., 2004b. ApJL 612, L93.